Subwavelength, binary lenses at infrared wavelengths

J. R. Wendt,[a] G. A. Vawter, R. E. Smith,[b] and M. E. Warren
Sandia National Laboratories, Albuquerque, New Mexico 87185-0603

(Received 29 May 1997; accepted 18 August 1997)

We describe the nanofabrication of subwavelength, binary lenses in GaAs for operation in the infrared. Subwavelength surface relief structures create an artificial material with an effective index of refraction determined by the fill factor of the binary pattern and can be designed to yield high-efficiency diffractive optical elements. In this work, we designed and fabricated a circular-aperture, off-axis lens with a deflection angle of 20°, focal length of 110 μm, and diameter of 80 μm, for operation at 975 nm. The off-axis lens design has a theoretical efficiency of 92% and the fabricated lens exhibits a diffraction efficiency into the first order of 72% and 59% of the transmitted power for TE and TM polarization, respectively. A significant advantage of these subwavelength structures is that fabrication requires only a single-lithography-and-etch-step process, in this case, electron-beam lithography and reactive-ion-beam etching. © *1997 American Vacuum Society.* [S0734-211X(97)13206-1]

I. INTRODUCTION

Subwavelength, binary lenses are an emerging technology in the field of high-diffraction-efficiency micro-optics, which exploit current capabilities in nanofabrication. The need for integrable micro-optics in the 1 μm wavelength regime is driven by the success of vertical-cavity surface-emitting lasers (VCSELs)[1] and applications such as high-speed optical interconnects in multichip modules.[2] Subwavelength, binary surface-relief structures are artificial materials with an effective index of refraction that can be tailored by varying the duty cycle of the binary pattern. Such structures also have interesting polarization-dependent properties[3] and allow the formation of antireflection surfaces.[4] To create a given lens with this technique, one must create a subwavelength pattern whose spatial variation of effective index of refraction matches that of the desired, ideal Fresnel zone lens equivalent, see Fig. 1. Subwavelength structures have the advantage of requiring only a single lithography and etch step for fabrication. By comparison, conventional, multilevel binary optics[5] only approximate the smooth phase profile of the Fresnel zones and require multiple lithographic and etch steps with stringent alignment tolerances. The main challenge in fabrication of the subwavelength structures at optical wavelengths is achieving the nanometer-scale dimensions, but this challenge is met by present capabilities of electron-beam lithography and various dry etching techniques. For more practical, cost-effective mass production of subwavelength optical elements, it may be possible to utilize a nanoimprinting technique[6] once a suitable master has been fabricated.

In this work, we describe the nanofabrication of subwavelength, binary lenses in GaAs for operation in the infrared. We have previously reported a high-efficiency, high-performance blazed grating,[7] which formed the basis for this work. There has been one report of an on-axis diffractive lens utilizing mostly subwavelength features,[8] but the lens design simply mimics a four-phase-level binary optic. To our knowledge, our present work is the first report of the design and fabrication of a true, zeroth-order subwavelength lens. Certainly, this is the most ambitious subwavelength structure in terms of form and function reported to date.

II. EXPERIMENT

We designed a fast off-axis subwavelength lens for fabrication in GaAs and for operation at 975 nm with normal incidence. The lens has a circular aperture, with a diameter of 80 μm, focal length of 110 μm, and deflection angle of 20°. Each Fresnel zone of the lens is generated by a single curved, subwavelength blazed grating element. For each zone, the number of line/space pairs is chosen such that the features are less than the wavelength of 975 nm light in GaAs (~280 nm). The off-axis lens is comprised of 25 zones. The outermost zone has a width of 1.7 μm and four line/space pairs and the innermost zone has a width of 14.7 μm and 45 line/space pairs. Because the features are only slightly smaller than the wavelength of light in the material, the design calculations are based on rigorous coupled wave analysis.[9] The technique allowed the use of optimization algorithms to arrive at a structure based on maximizing the power in the first diffracted order.[10] A unique feature of our design procedure is that we did not limit ourselves solely to either pulse-width or pulse-position modulation but rather, allowed both the width and spacing of the grating lines to vary in order to yield the most practically realizable design. It should be noted that for the largest zone of the lens (the zone corresponding to the central zone of an on-axis lens), the simple effective medium theory[11] was used because use of the optimization routine would have taken prohibitively long on the personal computer being used for the calculations. This approximation is not expected to affect the performance of the off-axis lens to a significant degree because the first zone is a small percentage of the overall lens area. The minimum dimensions of the lines and spaces were con-

[a]Electronic mail: jrwendt@sandia.gov
[b]Present address: RPI Japan, Inc., Yokohama, Japan.

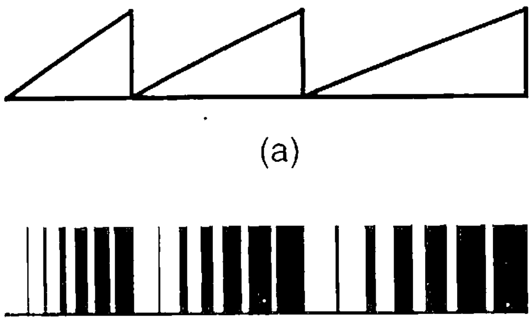

FIG. 1. Schematic cross section of a portion of (a) a Fresnel zone lens and (b) the equivalent subwavelength, binary lens.

strained to lie within our fabrication limits. Specifically, the minimum line dimension was set to 42 nm and the minimum space dimension was set to 100 nm. For the design etch depth of 540 nm, this results in a maximum aspect ratio of 12.8:1 for an etched line and 5.4:1 for an etched space. Without the flexible design and dimensional constraints, the most obvious design for a subwavelength blazed grating element would be a linear variation in the duty cycle of a line/space pair resulting in vanishingly small linewidths at the low index end and vanishingly small spaces at the high index end. The fact that subwavelength structures have polarization-dependent properties complicates the design of a general lens for use with light of mixed polarization. In this case, the optimization algorithm was set to maximize the transmission efficiency (into the first order) of each zone for a 50/50 weighted average of TE and TM polarization. The resulting design for the off-axis lens has a theoretical diffraction efficiency into the first order of 92% of the transmitted power compared to a maximum of 41% for a conventional two-phase-level diffractive optic. Eight-phase levels, requiring three lithography and etch steps, are necessary to achieve over 90% efficiency in a conventional binary optic. It may be noted that the same lens, designed solely for TE polarization, would have a theoretical efficiency greater than 92% while the same lens, designed solely for TM polarization, would have a theoretical efficiency less than 92%. For the lens design used in this work, the efficiency is expected to be greater for TE polarization than for TM polarization.

The stringent dimensional requirements of the above design were achieved using electron-beam lithography and reactive-ion-beam etching (RIBE) with a Ni/SiO_2 mask. Fabrication was performed on samples from a 3 in. diam. bulk GaAs wafer. The frontside of the wafer was coated first with 120 nm of plasma-deposited SiO_2 and then spin coated with 100 nm of polymethylmethacrylate (PMMA) electron-beam resist. Following electron-beam patterning of the PMMA, 5 nm of titanium (for adhesion) and 40 nm of nickel were evaporated onto the sample and the unwanted metal lifted off. The Ti/Ni pattern was transferred first into the SiO_2 layer by reactive-ion etching (RIE) and then into the GaAs surface by RIBE. The fabrication steps are described in more detail below.

The electron-beam lithography was performed on a JEOL JBX-5FE field-emission system operating at 50 kV. A beam current of 500 pA, with a corresponding beam diameter of 6 nm, was used. The addressed pixel spacing was 5 nm in an 80 μm field. The PMMA thickness of 100 nm was chosen to be as thin as possible for maximum resolution while still allowing for clean, reliable lift-off of the 45 nm evaporated Ti/Ni layer. To compensate for the proximity effect during exposure, resist deformation during metal evaporation, and any lateral dimension changes while transferring the Ti/Ni pattern to the SiO_2 and GaAs, the lens pattern was biased according to the same algorithm determined in the demonstration of the subwavelength blazed grating[7] with a bias value of 60 nm.

Each lens was written within a single 80 μm writing field of the JEOL instrument so that no field stitches are present in the exposed pattern. The best dose range for the lens was found to be 650–700 $\mu C/cm^2$. The patterns were developed for 1 min in a 1:3 solution of methyl isobutyl ketone (MIBK) and isopropyl alcohol (IPA). Empirical proximity correction was employed in portions of the first zone of the off-axis lens where the linewidths are relatively large and dense in comparison to the outer zones. After the Ti/Ni lift-off, the SiO_2 layer was etched using CHF_3/O_2 RIE. The SiO_2 layer serves as a well-behaved component of the etch mask and facilitates the removal of the Ti/Ni layer at the end of the fabrication sequence. The GaAs was etched in a custom-built RIBE system with an inductively coupled plasma (ICP) ion source. The etch gas was chlorine at a pressure of 3.5×10^{-4} Torr. The acceleration voltage and beam current density were 300 eV and 0.68 mA/cm^2, respectively. Etches were performed on a timed basis according to system calibration and accounting for etch lag effects.[12] A scanning electron micrograph of the cross section of four Fresnel zones of a fabricated subwavelength lens is shown in Fig. 2(a). A scanning electron micrograph of the cross section of a single Fresnel zone showing the detailed structure of the line/space pairs is shown in Fig. 2(b). The minimum feature size is 50 nm and the maximum aspect ratio is 12.8:1. As expected, there is etch depth variation across the zone pattern as a function of the etched groove width. The average etch depth measured across all the spaces of the zone shown in Fig. 2(b) is 535 nm, extremely close to the design depth of 540 nm. The variation in etch depth is $\pm20.5\%$ relative to the average etch depth. This is a significant variation and is expected to degrade the lens efficiency but two things should be noted. One, because these are subwavelength structures where the effective index as a function of position is related to the integrated average of the index over a small volume of the structure at a given position, the exact geometry of the subwavelength features is not important so long as the effective index profile matches the design. Two, the etch depth variation could be parameterized and included in the design optimization algorithm to compensate for the effect. For the purposes of this work, the etch depth variation is not a

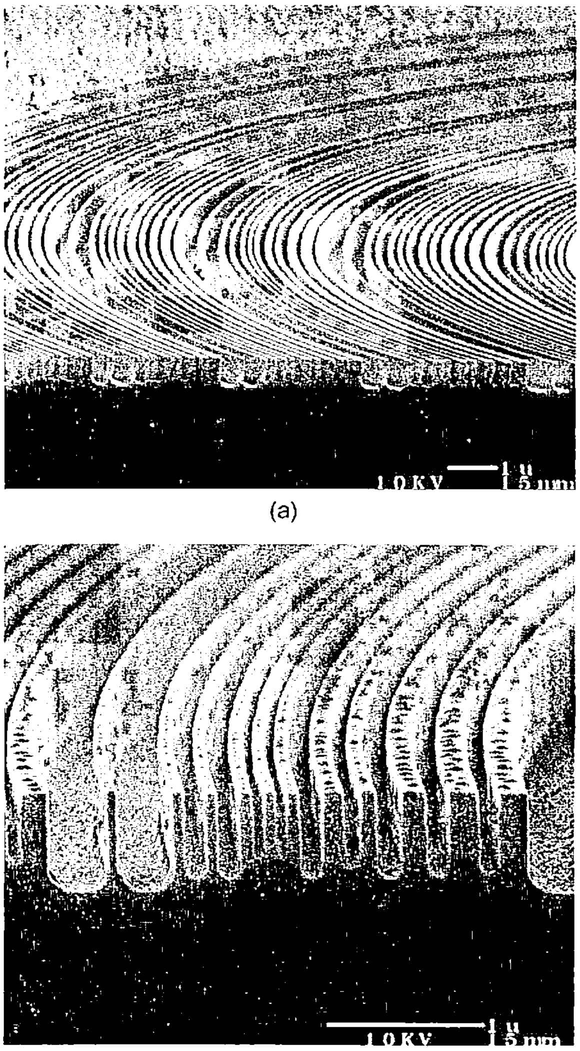

(a)

(b)

FIG. 2. Scanning electron micrograph of the cross section of (a) a portion of a fabricated subwavelength, binary lens in GaAs showing four Fresnel zones and (b) a single Fresnel zone of the lens showing the detail of the blazed ating element.

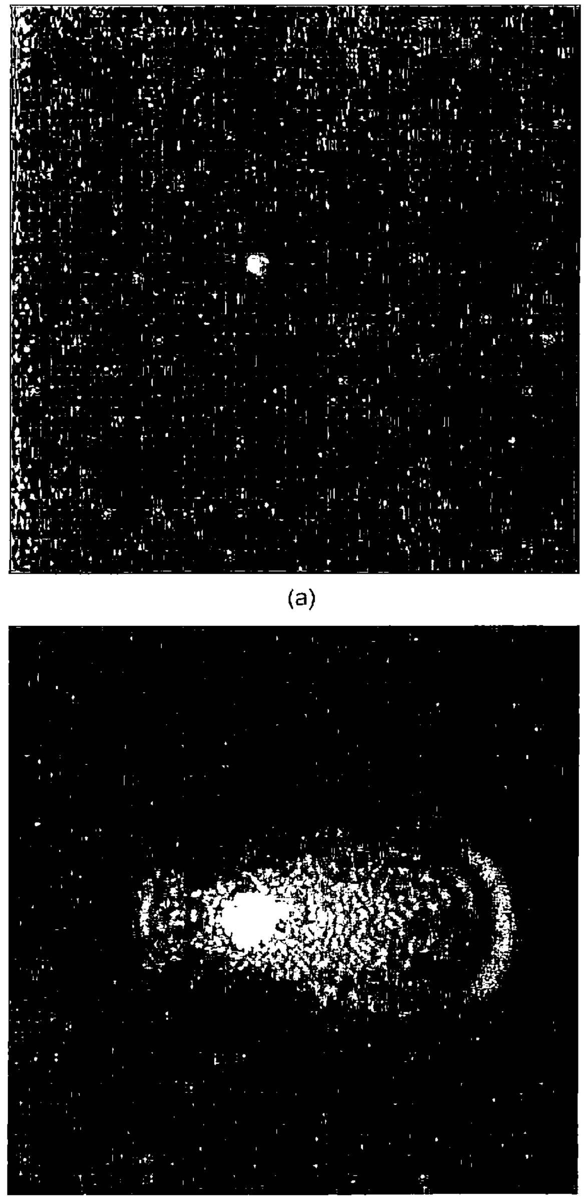

(a)

(b)

FIG. 3. Beam profile at the focal point for TE polarization for the off-axis lens as captured by a CCD camera (a) unsaturated, showing the 4 μm spot size and (b) saturated, showing the higher-order aberrations present at low levels.

significant enough problem to prevent demonstration of the functionality of the lens design.

III. RESULTS AND DISCUSSION

The diffraction efficiency of the lens was measured by the following technique. Light transmission was limited to the lens region by depositing a chrome aperture aligned precisely to the lens area. To measure the total transmitted power through the lens, an integrating sphere was aligned in close proximity to the lens to collect all transmitted light. To measure the transmitted power into the first diffracted order, the integrating sphere was aligned 20° off-normal and a pinhole with an effective diameter of 12 μm was aligned at the focal point of the lens. In each case, a reference detector was used to normalize out laser fluctuations. The diffraction efficiency for transmitted light into the first order measured by this technique is 72% for TE polarization and 59% for TM polarization, both respectable values but below the theoretical value of 92% for mixed polarization. The shortfall in measured efficiency compared to the predicted theoretical efficiency probably arises from the combination of several effects including deviations in the line/space dimensions and variation in etch depths across each of the blazed grating zone elements compared to the design values, the previously mentioned approximation used for the design of the first zone, and various random structural defects in the lens and deposited aperture. The beam-spot profile at the focus point of the lens was measured for TE polarization by a charge-coupled device (CCD) camera and is shown for two saturation levels in Fig. 3. The full width at half maximum as measured from the data shown in Fig. 3(a) is 4 μm, within a factor of 3 of the diffraction limit for the lens, which is 1.6 μm. Figure 3(b) shows the aberrations present at low levels in the focused beam. The aberrations can be attributed in part to an approximation used in the design of the lens. For each blazed zone of the lens, a linear phase profile was used instead of the ideal curved profile. This introduces higher-order aberrations in the resulting lens. The aberrations may also arise in part from any optical misalignment present in the measurement setup. Because the fabricated lens is very fast (f/1.3), its performance is very sensitive to alignment of the incident beam.

IV. SUMMARY

The nanofabrication of subwavelength, binary, high-efficiency diffractive lenses, operating at infrared wavelengths, has been demonstrated in GaAs utilizing electron-beam lithography and reactive-ion-beam etching. Successful fabrication of these structures was aided by constraining the design algorithm to dimensions and aspect ratios within the limits of our fabrication capabilities. The fabricated off-axis lens exhibited a diffraction efficiency of into the first order of 72% and 59% of the transmitted power for TE and TM polarization, respectively. This work demonstrates the potential for high-speed, high-efficiency lenses and other micro-optic elements fabricated in a single etch step and integrated with optoelectronic devices.

ACKNOWLEDGMENTS

The authors thank T. R. Carter and S. Samora for expert technical assistance and W. C. Sweatt for technical discussions. Sandia is a multiprogram laboratory operated by Sandia Corporation, a Lockheed Martin Company, for the United States Department of Energy under Contract No. DE-AG04-94AL85000.

[1]W. W. Chow, K. D. Choquette, M. H. Crawford, K. L. Lear, and G. R. Hadley, IEEE J. Quantum Electron. 33, 1810 (1997).
[2]R. F. Carson, M. L. Lovejoy, K. L. Lear, M. E. Warren, P. K. Siegal, D. C. Craft, S. P. Kilcoyne, and O. Blum, SPIE Crit. Rev. Opt. Sci. Technol. CR62, 35 (1996).
[3]D. C. Flanders, Appl. Phys. Lett. 42, 492 (1983).
[4]J. R. Wendt, G. A. Vawter, R. E. Smith, and M. E. Warren, J. Vac. Sci. Technol. B 14, 4096 (1996).
[5]G. J. Swanson and W. B. Veldkamp, Opt. Eng. (Bellingham) 28, 605 (1989).
[6]S. Y. Chou, P. R. Krauss, and P. J. Renstrom, J. Vac. Sci. Technol. B 14, 4129 (1996).
[7]J. R. Wendt, G. A. Vawter, R. E. Smith, and M. E. Warren, J. Vac. Sci. Technol. B 13, 2705 (1995).
[8]F. T. Chen and H. G. Craighead, Opt. Lett. 21, 177 (1996).
[9]M. G. Moharam and T. K. Gaylord, J. Opt. Soc. Am. 72, 1385 (1982).
[10]M. E. Warren, R. E. Smith, G. A. Vawter, and J. R. Wendt, Opt. Lett. 20, 1441 (1995).
[11]M. Born and E. Wolf, *Principles of Optics*, 6th ed. (Pergamon, New York, 1980).
[12]R. A. Gottscho, C. W. Jurgensen, and D. J. Vitkavage, J. Vac. Sci. Technol. B 10, 2133 (1992).